

Space Weather Application Using Projected Velocity Asymmetry of Halo CMEs

G. Michalek · N. Gopalswamy · S. Yashiro

Received: 3 March 2007 / Accepted: 10 January 2008 / Published online: 3 February 2008
© Springer Science+Business Media B.V. 2008

Abstract Halo coronal mass ejections (HCMEs) originating from regions close to the center of the Sun are likely to be responsible for severe geomagnetic storms. It is important to predict geoeffectiveness of HCMEs by using observations when they are still near the Sun. Unfortunately, coronagraphic observations do not provide true speeds of CMEs because of projection effects. In the present paper, we present a new technique to allow estimates of the space speed and approximate source location using projected speeds measured at different position angles for a given HCME (velocity asymmetry). We apply this technique to HCMEs observed during 2001–2002 and find that the improved speeds are better correlated with the travel times of HCMEs to Earth and with the magnitudes of ensuing geomagnetic storms.

Keywords Sun: solar activity · Sun: coronal mass ejections

1. Introduction

Halo coronal mass ejections (HCMEs) originating from regions close to the central meridian of the Sun and directed toward Earth cause the most severe geomagnetic storms (Gopalswamy, Yashiro, and Akiyama, 2007, and references therein). By using coronagraphic observations it is possible to determine the occurrence rate, direction of propagation in the plane of the sky, angular width, and speed (*e.g.*, Kahler, 1992; Webb *et al.*, 2000; St. Cyr *et al.*, 2000; Gopalswamy, Lara, and Yashiro, 2003; Gopalswamy, 2004; Yashiro *et al.*, 2004) of CMEs. It is well known that geoeffective CMEs originate mostly within a heliographic longitude of $\pm 30^\circ$ (Gopalswamy *et al.*, 2000, 2001; Webb

G. Michalek (✉)
Astronomical Observatory of Jagiellonian University, Cracow, Poland
e-mail: michalek@oa.uj.edu.pl

N. Gopalswamy
Solar System Exploration Division, NASA GSFC, Greenbelt, MD, USA

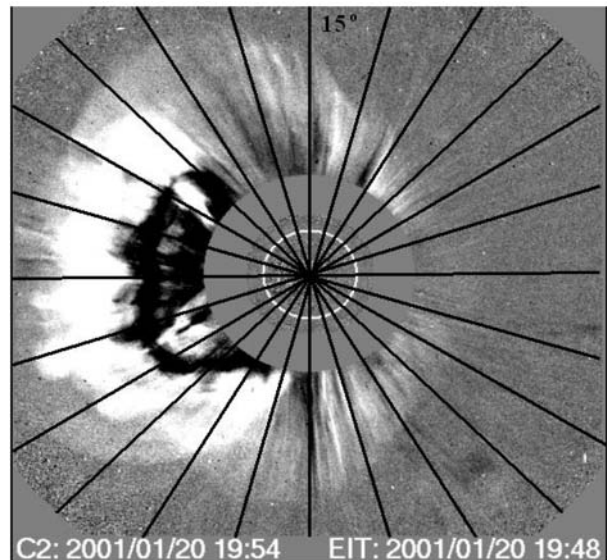
S. Yashiro
Center for Solar and Space Weather, Catholic University of America, Washington, DC, USA

et al., 2000; Wang, Sheeley, and Andrews, 2002; Zhang *et al.*, 2003) and that the initial speed of the CMEs is correlated with the Dst index (Tsurutani and Gonzalez, 1998; Srivastava and Venkatakrishnan, 2002; Yurchyshyn, Wang, and Abramenko, 2004). These studies were based on the plane of the sky speeds of CMEs without considering projection effects. Recently, there have been several attempts to correct for projection effects and determine the real CME parameters [Zhao, Plunkett, and Liu, 2002 (ZPL); Michalek, Gopalswamy, and Yashiro, 2003 (MGY); Xie, Ofman, and Lawrence, 2004 (XOL); Michalek, 2006 (M)]. These techniques, which need special measurements in coronagraphic fields of view, were based on the assumptions that CMEs have cone shapes and propagate with constant speeds. Based on the cone model, Michalek *et al.* (2006) demonstrated that fast CMEs originating on the western hemisphere close to the disk center are most likely to cause the most severe geomagnetic storms ($\text{Dst} \leq -150 \text{ nT}$), although there have been some east-hemisphere CMEs capable of causing such storms (Gopalswamy *et al.*, 2005a; Dal Lago *et al.*, 2006). Recently Moon *et al.* (2005) introduced a new direction parameter in correlation with geoeffectiveness of CMEs. It is defined as the ratio of the shortest to the largest distance of the CME front from the disk center for a given LASCO image. They demonstrated that this parameter is strongly correlated with the geoeffectiveness of CMEs. In this paper we present a new but similar technique to calculate the true speed of HCMEs, based on the differences in the projected speeds measured around the occulting disk. Our direction parameters are determined from several (4–5) LASCO images and should be more accurate in describing the asymmetry of HCMEs. We use the space speeds for the prediction of travel times (TTs) of HCMEs to Earth and to determine magnitudes (Dst index) of geomagnetic storms. The results obtained with this simple technique are compared with those from other methods (cone models). The paper is organized as follows: In Section 2, the technique used to determine the improved speeds is presented. In Section 3, the data considered for this study are described. In Section 4, we implement the improved speeds for space weather forecasting. Finally, conclusions are presented in Section 5.

2. Technique for the Speed Estimation

The sky-plane measurement describing the properties of CMEs, especially HCMEs, are subject to projection effects. However, true speeds in the direction of Earth are needed for estimating the travel times of CMEs to Earth (Gopalswamy *et al.*, 2001). This issue is crucial for space weather forecasting. We propose getting realistic speeds by determining an asymmetry ratio (ASR) in the projected speeds measured at different position angles around the occulting disk. The ASR is defined as the ratio between the maximum and minimum speeds measured at different position angles around the occulting disk for a given halo CME. A two-step procedure is carried out to obtain the ASR. First, by using height–time plots measurements every 15° the projected speeds were determined at 24 position angles (see Figure 1 for an illustration of the method). Next, from these values, we calculate running averages from four successive speeds around the occulting disk. This allowed us to get 24 average speeds around the occulting disk for each event. Thus the ASR is the ratio between the maximum ($\langle V_{\max} \rangle$) and minimum ($\langle V_{\min} \rangle$) average speeds determined this way. There are two reasons to use this procedure for determining ASRs. First, CMEs sometimes are irregular with narrow and fast structures that can overestimate the measured projected speeds. Second, CMEs can be faint and single measurements are prone to large errors. Our procedure minimizes these errors. It is important to note that the ASR has a real physical meaning. It is commonly assumed that CMEs have a cone shape,

Figure 1 An example HCME (20 January 2001) with dark lines along which the height–time measurements were performed.



which was described in detail in a few papers (Michalek, Gopalswamy, and Yashiro, 2003; Michalek, 2006; Xie, Ofman, and Lawrence, 2004). Thus this parameter obtained directly from coronagraphic observations should better indicate CME propagation directions than could be deduced from the associated flare locations. Such locations of CMEs are very useful for eliminating projection effects and for estimating the radial speeds and geoeffectiveness of CMEs. Moon *et al.* (2005) demonstrated that a direction parameter obtained from the asymmetry in the 3D shape of CMEs has a relatively good correlation with the geoeffectiveness of CMEs. Many halo CMEs have irregular shapes in the LASCO field of view, so the procedure proposed by Moon *et al.* (2005) is not accurate for such events. To minimize errors we propose determining the directional parameter in the velocity space from several (4–5) LASCO images. Following their consideration, we defined the ASR using the maximum ratio between these projected speeds for a given event. We assume that the improved speeds of CMEs could be expressed by the formula

$$V_{\text{imp}} = \langle V_{\max} \rangle + \langle V_{\max} \rangle / \text{ASR}, \quad (1)$$

where

$$\text{ASR} = \langle V_{\max} \rangle / \langle V_{\min} \rangle.$$

From these equations, we see that V_{imp} could be expressed as a simple sum of V_{\max} and V_{\min} . If a given CME originates at the limb then $V_{\min} = 0$ and the radial speed is exactly equal to V_{\max} . If the location of a given CME moves from the limb to the center of the Sun then V_{\max} decreases and V_{\min} increases. At the disk center, when HCMEs are symmetric, $V_{\min} = 2\langle V_{\max} \rangle$. It is not a perfect approximation of the radial speed but the only one possible because other methods do not work for symmetric HCMEs. The projection effects are mostly determined by the source locations and widths of CMEs. Unfortunately, in comparison to the cone models, our technique allows us to estimate only the source locations of CMEs.

3. Data

A list of HCMEs studied in this paper is displayed in Table 1. We considered only front-side full HCMEs during a period from the beginning of 2001 until the end of 2002. We selected this limited period of time to get a representative sample of HCMEs to test our new technique. In the considered period of time, 70 front-side full HCMEs were found in the SOHO/LASCO catalog. One of them was too faint to perform necessary measurements, so 69 front-side HCMEs are displayed in Table 1. Using data from World Data Center Kyoto (<http://swdcdb.kugi.kyoto-u.ac.jp>) we investigated geomagnetic disturbances caused by these events. To find a relationship between HCMEs and magnetic disturbances a two-step procedure was used. First, we found all geomagnetic storms, in the considered period of time, with $Dst \leq -30$ nT (a high limit chosen following Michalek *et al.*, 2006). We assume that the associated magnetic disturbance should start no later than 120 hours after the first appearance of a given event in the LASCO field of view and no sooner than the necessary travel time of a given CME to Earth calculated from the measured maximal projected speed. We related a given disturbance with a given HCME if they were within the specified time range. Twenty events from our list were not geoeffective ($Dst > -30$ nT). These HCMEs were slow ($V < 900 \text{ km s}^{-1}$) or originated closer to the solar limb. By examining solar wind plasma data (from the Solar Wind Experiment, Ogilvie *et al.*, 1995) and interplanetary magnetic field data [from the Magnetic Field Investigation (*Wind/MFI*) instrument, Lepping *et al.*, 1995], we identified interplanetary shocks driven by the respective interplanetary CMEs (ICMEs). Measuring the time when a HCME first appears in the LASCO field of view and the arrival time of the corresponding shock at Earth allows the travel time (TT) to be determined (e.g., Manoharan *et al.*, 2004; Gopalswamy *et al.*, 2005c).

The results of our considerations are presented in Table 1. The first column gives the date of the first appearance in the LASCO field of view. The next three columns display parameters obtained from the projected speeds ($\langle V_{\max} \rangle$, $\langle V_{\min} \rangle$, and ASR). In column 5 linear speeds from the SOHO/LASCO catalog are presented. The location of flares associated with CMEs are shown in column 6. In column 7 the minimum values of Dst indices for geomagnetic disturbances caused by HCMEs are displayed. Finally, in column 8 the travel times (TTs) of the shock to the Earth are presented. ASR varies from 1.11 to 7.59. The lowest values are for events close to the disk center. The highest values are for limb HCMEs. V_{\max} is close to the catalog speed (V) for most events. The difference arises from the fact that V_{\max} is obtained as an average over four position angles, whereas V is from a single position angle.

4. Space Weather Application

For space weather application it is crucial to predict, with good accuracy, the travel times (TTs) and strengths (Dst) of geomagnetic disturbances. In the next two subsections, we consider these issues using the improved speeds and the ASR parameter.

4.1. Prediction of the Onset of Geomagnetic Disturbances

Figure 2 shows the scatter plot of the plane of the sky speeds (from the SOHO/LASCO catalog) versus travel time. Correlation coefficients are 0.68 for the western and 0.50 for the eastern events. The standard error in determination of the TT is 16 hours. For comparison, we present a similar plot except that we use the improved speeds (Figure 3, left panel). The

Table 1 List of halo CMEs with the determined asymmetry ratio ASR.

Data	V_{\max} (km s $^{-1}$)	V_{\min} (km s $^{-1}$)	ASR	V (km s $^{-1}$)	Location	Dst (nT)	TT (hours)
2001/01/10	809	359	2.24	832	N13E36	–	–
2001/01/20a	850	384	1.98	839	S07E40	–61	66
2001/01/20b	1510	451	3.34	1507	S07E46	–61	64
2001/01/28	1090	311	3.50	916	S04W59	–40	68
2001/02/10	830	224	3.71	956	N37W03	–50	69
2001/02/11	1084	368	2.94	1183	N24W57	–50	50
2001/03/19	557	315	1.77	389	S20W00	–75	81
2001/03/24	973	325	2.99	906	N16E22	–56	72
2001/03/25	1020	276	3.69	677	N16E25	–87	67
2001/03/28	598	397	1.43	519	N18E02	–	–
2001/03/29	1021	773	1.32	942	N20W19	–387	38
2001/04/01	1462	262	5.58	1475	S22E90	–	–
2001/04/05	1447	607	2.38	1390	S24E50	–59	49
2001/04/06	1320	791	1.66	1270	S21E31	–63	64
2001/04/09	1118	581	1.92	1192	S21W04	–271	46
2001/04/10	2175	805	2.70	2411	S23W09	–271	33
2001/04/11	1179	396	2.97	1103	S22W27	–77	42
2001/04/12	1389	622	2.23	1184	S19W43	–75	35
2001/04/26	961	416	2.31	1006	N20W05	–47	41
2001/08/14	649	426	1.52	618	N16W36	–105	67
2001/08/25	1488	422	3.52	1433	S17E34	–	–
2001/09/11	755	305	2.47	791	N13E35	–	–
2001/09/24	2439	829	2.94	2402	S16E23	–102	34
2001/09/28	844	496	1.70	846	N10E18	–148	59
2001/10/01	1351	276	4.89	1405	S24W81	–166	55
2001/10/09	1030	467	2.20	973	S28E08	–71	54
2001/10/19a	906	593	1.52	901	N15W26	–187	48
2001/10/19b	605	166	3.64	558	N16W18	–	–
2001/10/22	1315	563	2.33	1336	S21E18	–57	35
2001/10/25	1080	530	2.03	1090	S16W21	–157	58
2001/11/01	457	138	3.30	453	N12W23	–	–
2001/11/03	555	247	2.24	457	N04W20	–	–
2001/11/04	1920	1729	1.11	1810	N06W18	–292	33
2001/11/17	1553	702	2.21	1379	S13E42	–48	54
2001/11/21	543	295	1.84	518	S14W19	–	–
2001/11/22a	1474	490	3.00	1443	S25W67	–221	35
2001/11/22b	1649	872	1.86	1437	S19W42	–221	33
2001/11/28	679	361	1.87	500	N04E16	–	–
2001/12/13	853	520	1.63	864	N16E09	–39	87
2001/12/14	1402	211	6.64	1506	N07E86	–39	39
2001/12/28	1920	362	5.31	2216	S24E90	–	–
2002/01/04	1205	357	3.36	896	N30E75	–	–
2002/01/14	1510	354	4.94	1492	S28W90	–	–

Table 1 (Continued.)

Data	V_{\max} (km s $^{-1}$)	V_{\min} (km s $^{-1}$)	ASR	V (km s $^{-1}$)	Location	Dst (nT)	TT (hours)
2002/02/20	835	236	3.50	952	N12W72	–	–
2002/03/10	1410	245	5.75	1429	S22E90	–	–
2002/03/11	953	234	4.07	950	S15E45	–	–
2002/03/14	961	299	3.21	961	S23E57	–37	93
2002/03/15	978	514	1.91	957	S08W03	–37	62
2002/03/18	958	393	2.43	989	S10W20	–	–
2002/03/22	1754	297	5.98	1750	S10W90	–100	39
2002/04/15	697	624	1.11	720	S15W01	–127	56
2002/04/17	1242	571	2.17	1240	S14W34	–149	60
2002/04/21	2374	560	4.24	2393	S14W84	–57	49
2002/05/07	637	255	2.50	720	S10E25	–110	79
2002/05/08	523	265	1.97	614	S12W07	–110	69
2002/05/16	612	228	2.67	600	S23E15	–58	67
2002/05/22	1612	565	2.85	1557	S30W34	–109	32
2002/07/15	1043	337	3.08	1151	N19W01	–	–
2002/07/18	926	389	2.38	1099	N19W30	–38	94
2002/07/20	1640	216	7.59	1941	S13E90	–38	32
2002/07/23	1717	327	5.25	2285	S13E72	–	–
2002/07/26	756	236	3.20	818	S19E26	–	–
2002/08/16	1466	691	2.12	1585	S14E20	–106	54
2002/08/22	928	201	4.58	998	S07W62	–45	106
2002/08/24	1886	804	2.34	1913	S02W81	–45	57
2002/09/05	1739	1028	1.69	1748	N09E28	–181	45
2002/11/09	1661	524	3.16	1838	S12W29	–43	48
2002/11/24	964	634	1.52	1077	N20E35	–64	50
2002/12/19	1050	549	1.91	1092	N15W09	–75	68

figures clearly show that the improved speeds are better correlated with the TT, with correlation coefficients being more significant: 0.72 for the western and 0.74 for the eastern events. The standard error in TT is 12 hours. The linear correlation coefficients are almost the same as those for the asymmetric cone model (Michalek, Gopalswamy, and Yashiro, 2007). For the M model the standard error was smaller by ~ 2 hours. To illustrate that our considerations are consistent with previous results we compare them with the ESA model (continuous line; Gopalswamy *et al.*, 2005b). For these plots we used only the 49 geoeffective ($\text{Dst} \leq -30$ nT) events. For comparison, in Figure 3 (right panel) we have added the three events (2000/07/14, 2003/10/28, and 2003/10/29) of historical importance, represented by the dark diamonds (Gopalswamy *et al.*, 2005b). In our list there are CMEs originating from close to the disk center and all the way to the limb. For arrival at Earth we need to consider Earth-directed speeds rather than the space speeds. We obtained the Earth-directed speeds for the 49 geoeffective events and plotted them in Figure 3 (right panel). We see that points agree well with the ESA model.

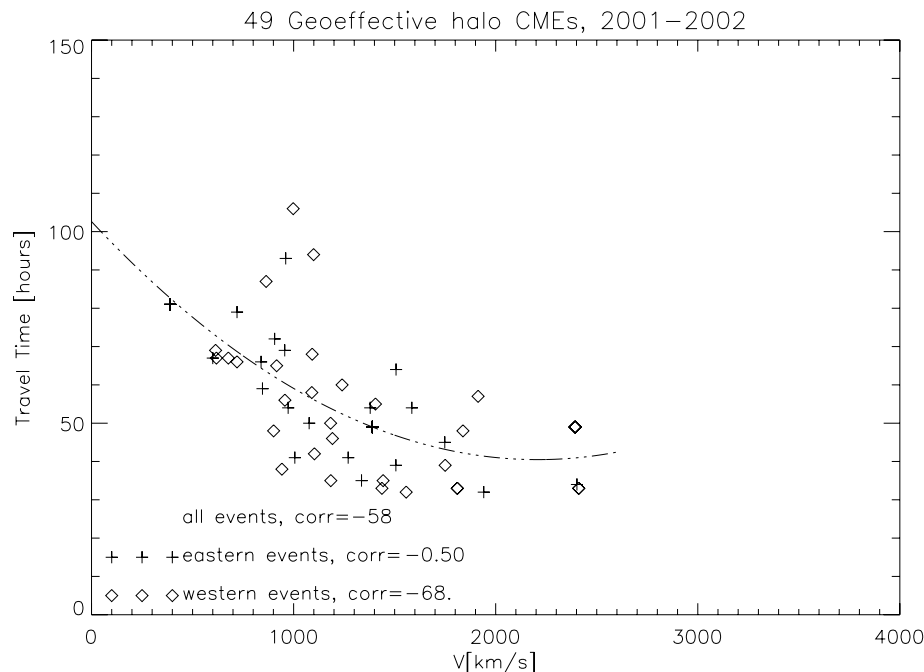


Figure 2 Scatter plot of plane of the sky speeds versus travel times (TT). Diamond symbols represent events originating from the western hemisphere and cross symbols represent events originating from the eastern hemisphere. The dot-dashed line is a second-degree polynomial fit to all the data points.

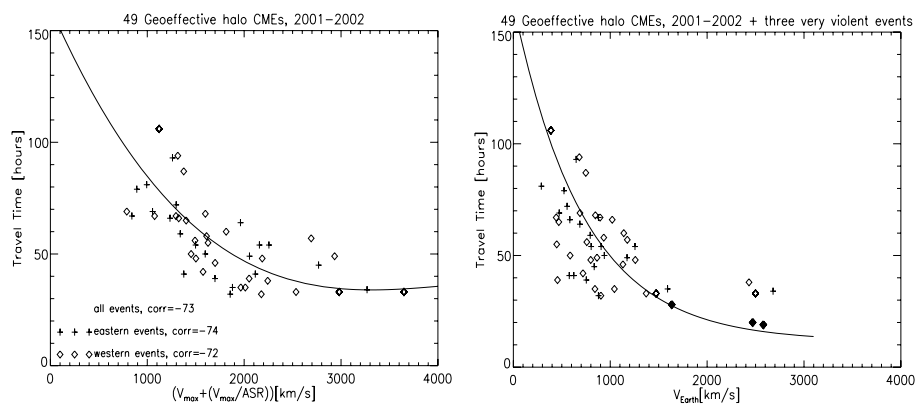


Figure 3 Scatter plots of the improved (left panel) and Earth-directed speeds (right panel) versus the HCME travel time (TT). Diamond and cross symbols represent events originating from the western and eastern hemispheres, respectively. The dot-dashed line (left panel) is a second-order polynomial fit to all the data points. The continuous line (right panel) is the ESA model representation. The three additional dark diamonds (only on the right panel) show the HCMEs (2000/07/14, 2003/10/28, and 2003/10/29) of historical importance.

4.2. Magnitudes of Geomagnetic Disturbances

Magnitudes of geomagnetic storms depend not only on the speeds of CMEs but also on the location of source region on the solar disk (*e.g.*, Moon *et al.*, 2005; Gopalswamy, Yashiro, and Akiyama, 2007). Michalek *et al.* (2006) found a significant correlation between Dst and $V\gamma$, where the parameter γ is the angular distance of a given CME from the plane of the sky. This parameter decides which part of a HCME hits Earth. Events with small γ strike Earth with their flanks whereas those with large γ hit Earth with their central parts. Figure 4 shows the scatter plots of the plane of the sky speeds multiplied by γ versus Dst index. The parameter γ was determined from the location of associated flares. There is a slight correlation between ($V\gamma$) and Dst. Correlation coefficients are approximately 0.49 for the western and 0.30 for eastern events, respectively. Locations of the associated flares could be different from locations of the associated CMEs. For comparison, Figure 5 shows a similar plot but for the improved speeds and the ASR parameters. We propose using the ASR instead of γ . This parameter includes source locations of CMEs (not flares) and should be more useful. There is only one difference from γ . Larger ASR means a location closer to the limb ($\gamma \sim 1/\text{ASR}$). Figure 5 shows the scatter plot of $((V_{\max}) + (V_{\max})/\text{ASR})/\text{ASR}$ versus Dst index. In other words, it is the scatter plot of improved speeds ($(V_{\max}) + (V_{\max})/\text{ASR} = V_{\text{imp}}$) multiplied by source locations ($1/\text{ASR} \sim \gamma$) versus Dst index. We used a similar formula in our previous paper (Michalek *et al.*, 2006). There is a significant correlation between $V_{\text{imp}}/\text{ASR}$ and Dst. Correlation coefficients are almost twice those obtained from the projected speeds: –0.65 for the western and –0.61 for eastern events, respectively. It is

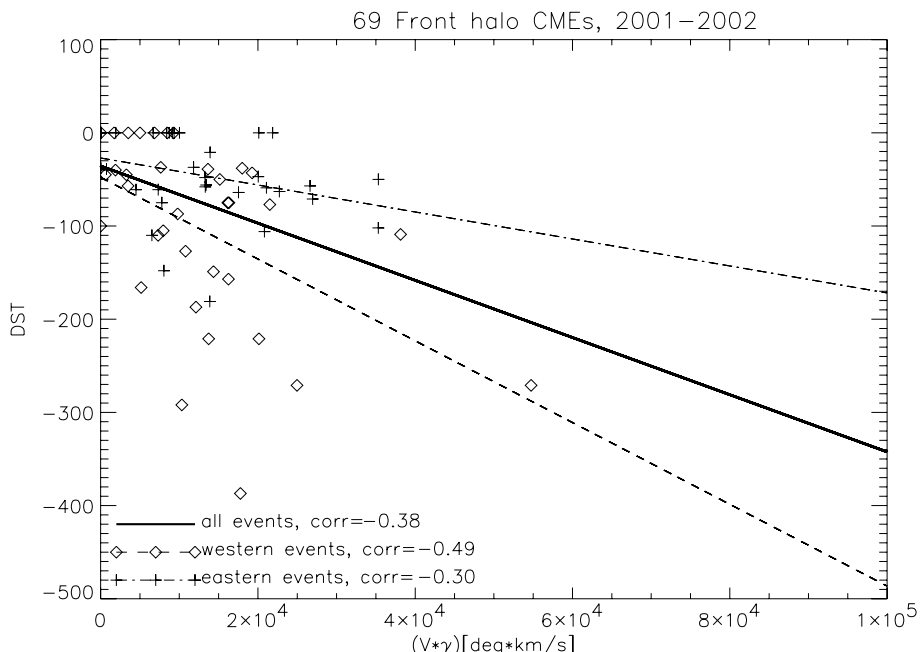


Figure 4 Scatter plot of plane of the sky speeds multiplied by γ versus Dst index. Diamond symbols represent events originating from the western hemisphere and cross symbols represent events originating from the eastern hemisphere. The solid line is a linear fit to all the data points, the dot-dashed line is a linear fit to western events, and the dashed line is a linear fit to eastern events.

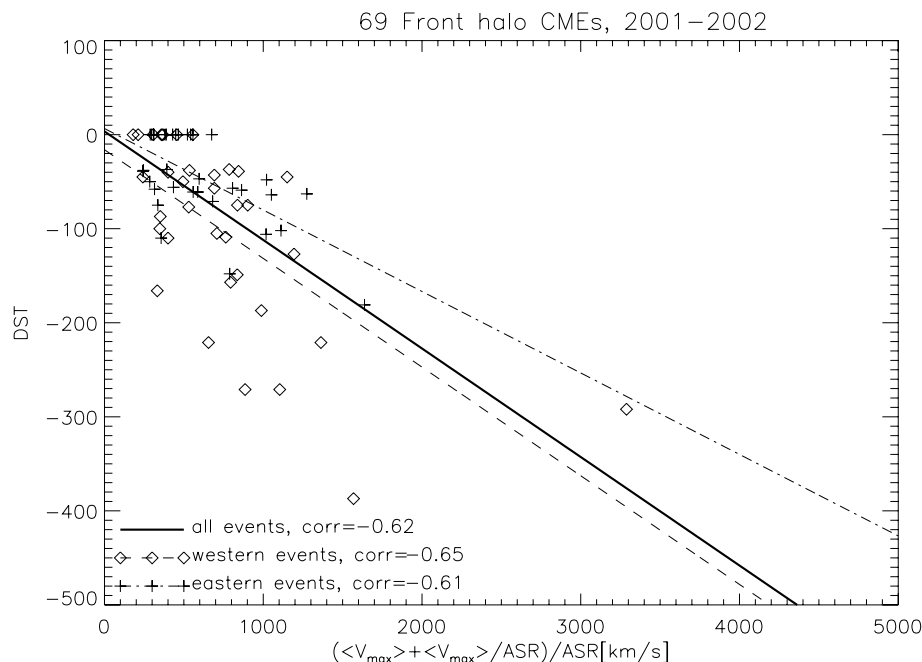


Figure 5 Scatter plot of $((V_{\max} + \langle V_{\max} \rangle) / \text{ASR}) / \text{ASR}$ versus Dst index. Diamond symbols represent events originating from the western hemisphere and cross symbols represent events originating from the eastern hemisphere. The solid line is a linear fit to all the data points, the dot-dashed line is a linear fit to the eastern events, and the dashed line is a linear fit to the western events.

clear that our technique could be very useful for space weather applications. For these plots (Figure 4 and Figure 5), we used all HCMEs from Table 1, even the nongeoeffective ones ($\text{Dst} > -30 \text{ nT}$). These events generate false alarms. Nongeoeffective HCMEs are slow ($V < 900 \text{ km s}^{-1}$) or have source region closer to the solar limb (see also Gopalswamy, Yashiro, and Akiyama, 2007). The correlation coefficients are slightly less significant in comparison to these received with the asymmetric cone model (Michalek, Gopalswamy, and Yashiro, 2007). In the case of the cone model the correlation coefficient for all events was -0.72 .

5. Summary

HCMEs are likely to cause severe geomagnetic storms. Speed is one of the most important parameters characterizing geoeffectiveness of CMEs. Unfortunately, coronagraphic observations, which provide CME speeds, are subject to projection effects. In this paper, we presented a new way to estimate the radial speeds of CMEs. For this purpose we introduced the asymmetry ratio (ASR), the parameter obtained from the maximum and minimum speeds measured at different position angles for a given event. This allowed us to estimate realistic radial speeds. In Figures 2 and 3 we compared the travel time (TT) prediction using the projected and improved speeds. Respective correlation coefficients clearly show that the improved speed allows us to predict the TT with better accuracy. The standard error is about 2 hours smaller for the improved speeds than for the projected speeds. A similar situation

appears when we compare correlation between speeds and source locations of CMEs and the strength of magnetic storms (Dst index). The correlation coefficients are about twice as large for improved speeds in comparison with the projected speeds (Figures 4 and 5). It is important to compare our results to previous considerations. Xie *et al.* (2006) calculated absolute differences between predicted (using the ESA model; Gopalswamy *et al.*, 2005b) and observed shock travel times for the cone models (XOL, MGY, and ZPL). They found that the mean errors for those models were 6.5, 12.8, and 9.2 hours, respectively. Recently, Michalek *et al.* (2007) calculated the same, but for the asymmetric cone model (with an error = 8.4 hours). In the present considerations, the mean difference between predicted (using a polynomial fit from Figure 2) and observed shock travel times is 10 hours, similar to the error from complicated cone models. Many authors demonstrated that the initial speeds of CMEs are correlated with the Dst index but the correlation coefficients were not significant because they applied the plane of the sky speeds. Using the MGY model, Michalek *et al.* (2006) showed that the correlation between the space speed of HCMEs and Dst index could be much more significant (their correlation coefficient was ~ 0.60). Recently, Michalek, Gopalswamy, and Yashiro (2007) showed that for the asymmetric cone model the correlation coefficient for the western events could be very significant (0.85). In the present study we found a correlation coefficient of 0.65 for the western events. Because in the present study we performed more accurate measurements of the projected speeds we got better results in comparison to the MGY model. Unfortunately, we do not involve the width of CMEs so we can only estimate the radial speeds of CMEs and our results are not as accurate as those of the asymmetric cone model (M). There are two important advantages of this method. First, this technique is very fast. To get the ASR we need only to determine the height – time plots from coronagraphic observations. We used the average maximum and minimum speeds obtained from four successive measurements running around the occulting disk. Second, we do not apply any model or assumptions. The method also has some weak points. Faint HCMEs cannot be used for the study, because it is difficult to get the height – time plots around the occulting disk. Fortunately poor events are generally not geoeffective so they are not of immediate concern. In contrast to the cone models we cannot estimate the widths of HCMEs. Neglecting this parameter may lead to overestimation of the radial speeds. Although we obtained very accurate results using very simple considerations it is important to note that CMEs have very complicated 3D structure (Cremades and Bothmer, 2004) and more factors may have to be included when determining their geoeffectiveness.

Acknowledgements This work was supported by NASA LWS T&T and SR&T grants. Work done by GM was supported in part by MNiSW through Grant No. N203 023 31/3055. SY was supported in part by NASA (NNG05GR03G).

References

- Cremades, H., Bothmer, V.: 2004, *Astron. Astrophys.* **422**, 307.
- Dal Lago, A., Gonzales, W.D., Balmaceda, L.A., Vieira, L.E., Echer, E., *et al.*: 2006, *J. Geophys. Res.* **111**, 14.
- Gopalswamy, N.: 2004, In: Poletto, G., Suess, S. (eds.) *The Sun and the Heliosphere as an Integrated System, ASSL Series*, Kluwer, Boston, 201.
- Gopalswamy, N., Lara, A., Yashiro, S.: 2003, *Astrophys. J.* **598**, L63.
- Gopalswamy, N., Yashiro, S., Akiyama, S.: 2007, *J. Geophys. Res.* **112**, A06112.
- Gopalswamy, N., Lara, A., Lepping, R.P., Kaiser, M.L., Berdichevsky, D., St. Cyr, O.C.: 2000, *Geophys. Res. Lett.* **27**, 145.
- Gopalswamy, N., Yashiro, S., Kaiser, R.A., Howard, R.A., Bougeret, J.-L.: 2001, *J. Geophys. Res.* **106**, 292907.

- Gopalswamy, N., Yashiro, S., Michalek, G., Xie, H., Lepping, R.P., Howard, R.A.: 2005a, *Geophys. Res. Lett.* **32**, L12S09 S09.
- Gopalswamy, N., Yashiro, S., Liu, Y., Michalek, G., Vourlidas, A., Kaiser, M.L., Howard, R.A.: 2005b, *J. Geophys. Res.* **110**, A09S15 S15.
- Gopalswamy, N., Barbieri, L., Lu, G., Plunkett, S.P., Skoug, R.M.: 2005c, *Geophys. Res. Lett.* **32**, L03S01.
- Kahler, S.W.: 1992, *Annu. Rev. Astron. Astrophys.* **30**, 113.
- Lepping, R.P., Acuna, M.H., Burlaga, L.F., Farrell, W.M., Slavin, J.A., *et al.*: 1995, *Space Sci. Rev.* **71**, 207.
- Manoharan, P.K., Gopalswamy, N., Yashiro, S., Lara, A., Michalek, G., Howard, R.A.: 2004, *J. Geophys. Res.* **109**, A06109.
- Michalek, G.: 2006, *Solar Phys.* **237**, 101.
- Michalek, G., Gopalswamy, N., Yashiro, S.: 2003, *Astrophys. J.* **584**, 472.
- Michalek, G., Gopalswamy, N., Yashiro, S.: 2007, *Solar Phys.* **246**, 399.
- Michalek, G., Gopalswamy, N., Lara, A., Yashiro, S.: 2006, *Space Weather J.* **4**, Cite ID S10003.
- Moon, Y.-L., Cho, K.-S., Dryer, M., Kim, Y.-H., Bong, S., Chae, J., Park, Y.D.: 2005, *Astrophys. J.* **624**, 414.
- Ogilvie, K.W., Chornay, D.J., Fritzenreiter, R.J., Hunsaker, F., Keller, J., *et al.*: 1995, *Space Sci. Rev.* **71**, 55.
- Srivastava, N., Venkatakrishnan, P.: 2002, *Geophys. Res. Lett.* **29**, 101029.
- St. Cyr, O.C., Howard, R.A., Sheeley, N.R., Plunkett, S.P., Michels, D.J., *et al.*: 2000, *J. Geophys. Res.* **105**, 18169.
- Tsurutani, B.T., Gonzalez, W.D.: 1998. In: *Geophys. Monogr.* **98**, AGU, Washington, 77.
- Wang, Y.M., Sheeley, N.R., Andrews, M.D.: 2002, *J. Geophys. Res.* **107**, 1340.
- Webb, D.F., Cliver, R.W., Crooker, N.U., Cyr, O.C., Thompson, B.J.: 2000, *J. Geophys. Res.* **105**, 7491.
- Xie, H., Ofman, L., Lawrence, G.: 2004, *J. Geophys. Res.* **109**, 03109.
- Xie, H., Gopalswamy, N., Ofman, L., St. Cyr, O.C., Michalek, G., Lara, A., *et al.*: 2006, *Space Weather J.* **4**, 10002.
- Yashiro, S., Gopalswamy, N., Michalek, G., St. Cyr, O.C., Plunkett, S.P., Rich, N.B., Howard, R.A.: 2004, *J. Geophys. Res.* **109**, 07106.
- Yurchyshyn, V., Wang, H., Abramenko, V.: 2004, *Space Weather J.* **2**(2), CiteID S02001.
- Zhang, J., Dere, K.P., Howard, R.A., Bothmer, V.: 2003, *Astrophys. J.* **582**, 520.
- Zhao, X.-P., Plunkett, S.P., Liu, W.: 2002, *J. Geophys. Res.* **107**, 1223.